World Electric Vehicle Journal

MDPI

Article

Mass, Centre of Gravity Location and Inertia Tensor of Electric Vehicles: Measured Data for Accurate Accident Reconstruction

Giorgio Previati †, Gianpiero Mastinu † and Massimiliano Gobbi *,†

Department of Mechanical Engineering, Politecnico di Milano, Via La Masa 1, 20156 Milan, Italy; giorgio.previati@polimi.it (G.P.); gianpiero.mastinu@polimi.it (G.M.)

* Correspondence: massimiliano.gobbi@polimi.it

† These authors contributed equally to this work.

Abstract: Accurate accident reconstruction requires the knowledge of the mass properties of vehicles, namely the centre of gravity location, the mass and the inertia tensor. Such data are seldom available, especially in case of newly produced electric vehicles. In this paper, vehicle inertia measurements, performed at Politecnico di Milano, refer to a number of electric vehicles. In addition to the "simple" measurement of vehicle inertia, measured mass properties are analysed to derive the proper empirical formulae for the estimation of the centre of gravity height and the moments of inertia. Both internal combustion and electric vehicles are considered. Data show a significant difference in the mass properties of the two types of vehicles. The proposed formulae can be effectively employed to quickly obtain a reasonable estimation of the mass properties of any vehicle. The results show that electric vehicles are characterised by higher values of mass with respect to internal combustion vehicles, but they present a lower centre of gravity location and proportionally lower values of the moments of inertia.

Keywords: mass properties; centre of gravity; inertia tensor; electric vehicles; accident reconstruction

Citation: Previati, G.; Mastinu, G.; Gobbi, M. Mass, Centre of Gravity Location and Inertia Tensor of Electric Vehicles: Measured Data for Accurate Accident Reconstruction. *World Electr. Veh. J.* **2024**, *15*, 266. https://doi.org/10.3390/wevj15060266

Academic Editor: Qiqi Li

Received: 20 May 2024
Revised: 10 June 2024
Accepted: 14 June 2024
Published: 17 June 2024

1. Introduction

Dynamic simulation is exploited in a wide range of situations to understand vehicle behaviour. During the design phase, dynamic simulation enables the early prediction of vehicle handling and comfort performance. The active and passive safety of a vehicle can also be virtually assessed. Through dynamic simulations, the tuning of vehicle settings can be refined and expedited. Among all these applications, a particularly crucial field were vehicle simulation plays a primary role is the reconstruction of automotive accidents.

In a world where about 1.3 million deaths and 20 to 50 millions injuries are related to traffic accidents each year [1], understanding the causes and dynamics of such accidents is of paramount importance to implement effective preventive and mitigating actions. Additionally, as each accident implies a tragedy for those involved, these individuals deserve an accurate reconstruction of what happened to correctly assess the moral and legal responsibilities.

The aim of accident reconstruction is the determination of the initial position and velocity of all vehicles and objects involved, as well as their motion to reach the rest position [2]. Although electronic and digital devices, both on board of vehicles and on the infrastructure, can provide recordings and data related to most accidents; this information can be misleading if not supported by the required computation and the understanding of their limits and uncertainties [3]. Furthermore, accident reconstruction is the only available tool when such recordings are not available.

Vehicle dynamic simulation requires knowledge of several vehicle parameters. Among these, mass properties (mass, centre of gravity location and inertia tensor) significantly affect the dynamic behaviour of vehicles [4]. Therefore, accurate knowledge of these parameters is essential for reliable simulations and to ensure better agreement between

simulated and experimentally measured real dynamic behaviour [5]. In the context of accident reconstruction, in [3], it is pointed out that if the rotational inertia of the vehicle is neglected, i.e., vehicles are treated as point masses, errors of about 100% can be introduced in the computation of the initial velocities of the vehicles. When more complex models are employed and vehicle moments of inertia are considered, errors in estimating these values impact the reconstructed dynamics of the involved vehicles. The authors of [6] demonstrated that in 2D planar impact models, the yaw moment of inertia influences both the preimpact velocities and postimpact trajectories of the vehicles. Comparable findings are presented in [7], thus showing that for specific accident dynamics, errors of 10% in the yaw moment of inertia or of 100 mm in the longitudinal position of the centre of gravity can lead to variations of up to 20% in preaccident velocities. Vehicle rollover is primarily influenced by the centre of gravity height and the roll moment of inertia [3,8,9]. Ref. [10] shows that a 50% change in the roll moment of inertia reduces about 40% of the dynamic rollover limit of a vehicle.

Mass properties, however, are seldom known or readily available. Their experimental determination is not straightforward. Only the mass and in-plane centre of gravity location can be easily measured. Measurement standards solely exist for the mass and centre of gravity location [11,12]. Determining the inertia tensor necessitates special, complex, and costly dedicated test rigs [13–15]. Two distinct approaches are employed for measuring the mass properties of rigid bodies. In the first approach, the moments of inertia are measured one at a time. In this case, different methods are usually employed for the the measurement of the roll and pitch moments of inertia or for the yaw moment of inertia. In [16,17], pendulums were used to swing heavy and large military vehicles around the roll and pitch axes. For the yaw moment of inertia, torsion pendulums [16] or multifilar pendulums [18] are often employed to induce oscillations around a vertical axis. In the second approach, all moments of inertia, and in some cases the location of the centre of gravity as well, are measured in a single test. In these methods, the body under investigation undergoes complex motion in space, and suitable identification procedures are used to derive the mass properties. In [19,20] K and C (Kinematics and Compliance) test beds were modified to identify the mass properties of whole cars, car subsystems and truck cabs. In [21,22], dynamic actuators were used to move a platform carrying the car. In [7], a multifilar pendulum was used to realise a highly nonlinear and complex motion of a frame carrying full vehicles or vehicle components. Yet, the described equipment are not widely available and only seldom employed [23].

Alternatively, the mass properties could be derived from 3D models of the vehicle. This deviation is not quite accurate, despite simplified model-based estimations of the centre of gravity location being used in the vehicle preliminary design stage [24]. Vehicles are composed of a large number of components (nearly thirty-thousand for internal combustion powered vehicles and more than one hundred thousand for electric vehicles). Even if very accurate and complex models of vehicle subsystems are available, only rough estimations of the mass properties can be obtained.

In some cases, complex, though less accurate, onboard systems for mass properties estimation can be developed for the estimation of such parameters [25].

Often, neither of the two considered options is available. In this case, the mass properties must be estimated. In the literature, some papers dealing with empiric formulae for the estimation of mass properties for cars are available. A quite large collection of vehicle mass properties can be found in [26–28]. These papers also provide some empiric formulae to be used for the estimation of the mass properties. The papers, however, refer mostly to vehicles from the USA market produced before 1998. Empiric formulae referring to easily available vehicle data, such as the mass, length, wheelbase, track, roof height and so on, have also been proposed by other authors and based on these databases [4,6,23,29,30]. More recently, the authors published simple empirical formulae based on vehicle mass properties referring to European market vehicles produced up to 2016 [31,32]. Formulae for estimating the mass, centre of gravity location and moment of inertia of cars can also

be found in [33]. In this paper, a series of estimating equations has been derived based on physical considerations and adapted to different car configurations (such as car type, front- or rear-wheel drive and so on). The derived set of equations and correction factors have been compared with available experimental data.

All of the considered databases refer almost exclusively to Internal Combustion (IC) vehicles. The diffusion of both pure electric (BEVs) and hybrid vehicles is increasing year by year. Such vehicles have completely different powertrains, thus resulting in very different mass distributions. Empirical formulae derived for IC vehicles may not directly apply, and their employment may lead to large estimation errors on the mass properties of BEVs.

This paper aims to address the lack of information regarding the mass properties of Battery Electric Vehicles (BEVs). From an engineering standpoint, having reliable formulae for the quick estimation of BEVs mass properties can significantly enhance the accuracy of simulations and accident reconstructions. Moreover, from a scientific perspective, the paper compares the mass properties of BEVs with those of traditional Internal Combustion (IC) vehicles. This comparison sheds light not only on the current trend of vehicle mass increase but also on how mass is distributed in new vehicles, especially considering the impact of larger batteries on the centre of gravity height and moments of inertia. This information can be beneficial not only for accident reconstruction, but also for vehicle design and control, especially for new electric vehicle architectures [34]. To achieve these objectives, the paper extends the existing database, previously presented in [31,32], by incorporating the data on more recent IC vehicles and a variety of BEVs. The two sets of mass properties, one for IC vehicles and the other for BEVs, are then compared, thus leading to the formulation of dedicated empirical formulae for each vehicle type.

This paper is organised as follows. The Section 1 is devoted to the description of the InTenso+ System of the Politecnico di Milano employed for the measurement of the vehicle mass properties considered in the paper. Then, a correlation analysis is presented to identify the most relevant vehicle parameters for the estimation of the centre of gravity height and of the moments of inertia. Finally, the interpolation formulae are presented, and the mass properties of IC vehicles and BEVs are compared.

2. InTenso+ System

The Intenso+ System, developed at the Politecnico di Milano, is designed for measuring the mass, centre of gravity location and inertia tensor of rigid bodies. The method has been presented in a series of papers [7,35,36], with particular reference to the measurement of the mass properties of vehicles. Figure 1 shows the two test rigs located at the LaST laboratory (Laboratory for Safety in Trasportation) of the Politecnico di Milano. On the left, the test rig for the measurement of full-scale vehicles is depicted, while on the right, the test rig for the measurement of vehicle subsystems is shown.

The measurement involves displacing the multibar pendulum carrying the body under investigation from a state of rest. The following complex motion is recorded using encoders and load cells, which are placed on the universal joints connecting the support bars to the ceiling frame. These measurements enable the reconstruction of the kinematic quantities describing the system's motion and the applied forces. Subsequently, through a proper mathematical procedure, the centre of gravity location and the components of the inertia tensor are identified.

The specifications of the test rigs are reported in Table 1. Details on the calibration and verification procedures can be found in [7,36].

Table 1. Technical specifications of the test rigs.

		InTenso+	**InTensino+**
Payload range	[kg]	500–3500	50–400
Maximum dimensions of the body ($L \times W \times H$)	[m]	$7 \times 2 \times 1.6$ (*)	$3 \times 1 \times 1$ (*)
Motion frequency	[Hz]	<5	<5

Table 1. *Cont.*

		InTenso+	InTensino+
Peack acceleration during test (min–max)	[m/s^2]	2–10	3–10
CoG uncertainty (in plane, height)	[mm]	±3 (**)–±5	±1.5–±3
Moment of inertia (MOI) uncertainty	[%]	±1%	±1%
Products of inertia (POI) uncertainty (% of the maximum MOI of the body)	[%]	±0.5%	±0.5%
MOI and POI resolution (% of the maximum MOI of the body)	[%]	0.2%	0.2%
Testing time (***)	[minutes]	<10	<10

(*) Dimensions are indicative. Fully customised fixturing can be realised. (**) Static balancing method. (***) The testing time does not consider the time needed to position the body on the test rig.

Figure 1. InTenso+ system of Politecnico di Milano. (**a**) Equipment for full vehicles (max 3500 kg). (**b**) Equipment for vehicle subsystems (up to 400 kg).

3. Vehicle Mass Properties Database

The mass properties data of several vehicles measured by the InTenso+ test rig have been collected into a database. The database comprises the mass properties of fifty-nine vehicles produced from 1997 to 2023. Forty-one are IC vehicles, while eighteen are BEVs. The database includes a wide variety of cars comprising small urban vehicles, medium and premium cars, as well as high performances sports cars. In Tables 2 and 3, the ranges of parameters covered by the vehicle database for IC vehicles and BEVs are reported. For confidentiality reasons, such data can be published only in the aggregated form. For the purposes of the present paper, this is not a limitation, as the paper is focused on the analysis of global formulae and not on the analysis of the mass properties of any given vehicle.

The vehicle data will be used in the following of the paper to focus on four mass properties, namely the centre of gravity height (CoG) and the three moments of inertia (MOI) along the three geometrical axes of the vehicle (longitudinal, lateral and vertical). The in-plane location of the centre of gravity was not considered, as it can usually be quite easily estimated from the axle loads of the car. The products of inertia were not considered, even though they are important for a correct simulation of the motion, as they strongly depend on the actual vehicle and its suspension configuration.

Table 2. Ranges of IC vehicle data.

Parameter	Units	Min. Value	Max. Value
Mass	[kg]	858	2363
Centre of gravity height *	[mm]	288	694
Jxx **	[kgm^2]	274	944
Jyy **	[kgm^2]	943	4802
Jzz **	[kgm^2]	1055	5033
Length	[mm]	3500	5262
Width	[mm]	1600	2035
Roof height	[mm]	1182	1699
Wheelbase	[mm]	2300	3171
Average track	[mm]	1402	1725
Power	[kW]	50	610
Max velocity	[km/h]	140	380
Year	[-]	1997	2023

* With respect to road plane. ** Reference system: x longitudinal, y lateral z vertical. Jxx, Jyy and Jzz indicate the roll, pitch and yaw MOI, respectively. Values refer to the centre of gravity.

Table 3. Ranges of BEV data.

Parameter	Units	Min. Value	Max. Value
Mass	[kg]	1644	2938
Centre of gravity height *	[mm]	453	601
Jxx **	[kgm^2]	679	1234
Jyy **	[kgm^2]	2410	5798
Jzz **	[kgm^2]	2579	5798
Length	[mm]	4584	5216
Width	[mm]	1852	2254
Roof height	[mm]	1445	1721
Wheelbase	[mm]	2720	3210
Average track	[mm]	1558	1720
Power	[kW]	151	484
Max velocity	[km/h]	180	250
Year	[-]	2017	2023

* With respect to road plane. ** Reference system: x longitudinal, y lateral z vertical. Jxx, Jyy and Jzz indicate the roll, pitch and yaw MOI, respectively. Values refer to the centre of gravity.

4. Correlation Analysis

Six easily available vehicle parameters were considered for the interpolation of the considered mass properties; namely, they are the following:

- Mass;
- Length;
- Width,
- Roof height,
- Wheelbase,
- Average track.

To verify if these parameters were actually independent, in Table 4, the correlation coefficients computed for these parameters considering the vehicles in the database are shown. The correlation coefficients were computed considering the nonlinear Spearman correlation [37]. This coefficient measures the strength and direction of a monotonic relationship between two ranked variables. The method did not assume any linear relationship or variable distribution and was robust to outliers.

From the correlation analysis reported in Table 4, it can be observed that the mass was correlated with all other parameters except the roof height, with a relatively high correlation with the length and especially the wheelbase. Also, the in-plane parameters were mostly correlated with each other. This observation is not surprising, considering that as vehicle

dimensions increase, they tend to grow both longitudinally and laterally, thus resulting in an increase in mass as well. Among all these correlations, the two correlations between the length, wheelbase, width and average track were particularly high, thus being above 0.9. Considering such high correlations, the wheelbase and average track were removed from the analysis, and only the length and width were considered.

In Table 5, the correlations between the vehicle parameters and mass properties are reported. The mass was strongly correlated with all the moments of inertia, but not with the centre of gravity height. The moments of inertia were also correlated, with different degrees of correlation, with the vehicle dimensions. THe centre of gravity height appeared to be correlated only with the roof height. Based on this analysis, approximation formulae for the moments of inertia should consider the mass and vehicle dimensions, while for the centre of gravity height, only the roof height seemed to be a relevant parameter. Additionally, all the relevant parameters had a positive correlation with the correlated mass properties, thus indicating that as one considered parameter increased, the correlated mass properties increased as well.

Finally, Table 6 shows the correlation coefficients among the considered mass properties. As expected, the moments of inertia were strongly correlated with each other, with an extremely high correlation between the pitch and yaw moments of inertia. The centre of gravity height was not correlated with any other considered mass parameter.

Table 4. Correlation analysis of vehicle parameters. In bold are the correlation coefficients with values higher than 0.8. RH is roof height, WB is wheelbase and AT is average track.

	Mass	**Length**	**Width**	**RH**	**WB**	**AT**
Mass	1	**0.80**	0.69	0.55	**0.87**	0.69
Length	**0.80**	1	0.75	0.37	**0.91**	0.76
Width	0.69	0.75	1	0.12	0.68	**0.93**
RH	0.55	0.37	0.12	1	0.48	0.16
WB	**0.87**	**0.91**	0.68	0.48	1	0.70
AT	0.69	0.76	**0.93**	0.16	0.70	1

Table 5. Correlation analysis between vehicle parameters and mass properties. In bold are the correlation coefficients with values higher than 0.8.

	CoG Height	**Roll MOI**	**Pitch MOI**	**Yaw MOI**
Mass	0.10	**0.93**	**0.96**	**0.96**
Length	0.05	0.72	**0.87**	**0.86**
Width	−0.25	0.55	0.68	0.69
Roof height	0.71	0.70	0.59	0.58

Table 6. Correlation analysis of vehicle mass properties. In bold are the correlation coefficients with values higher than 0.8.

	CoG Height	**Roll MOI**	**Pitch MOI**	**Yaw MOI**
CoG Height	1	0.28	0.22	0.20
Roll MOI	0.28	1	**0.93**	**0.93**
Pitch MOI	0.22	**0.93**	1	**0.996**
Yaw MOI	0.20	**0.93**	**0.996**	1

5. Formulae for the Centre of Gravity Height

The correlation analysis discussed in the previous section shows that the centre of gravity height was correlated to the roof height only. Therefore, the approximation formulae will be functions of only this vehicle parameter. This result is consistent with previously published formulae [4], where a linear interpolation with an intercept was used. In order to verify the order of interpolation, in Table 7, the *p*-values for the parameters in the case of linear interpolation without an intercept, linear interpolation with an intercept and quadratic interpolation are reported. From the results of the analysis, both for IC vehicles and for BEVs, the only term showing a *p*-value below 0.05 was the linear term.

Table 7. *p*-values for the parameters of different formulae for centre of gravity height estimation.

	Linear Model with Intercept	**Linear Model without Intercept**	**Quadratic Model with Intercept**
Model *	$CoG_z = a + b \cdot h_r$	$CoG_z = b \cdot h_r$	$CoG_z = a + b \cdot h_r + c \cdot h_r^2$
***p*-values—IC vehciles** **	$pv_a = 0.620$ $pv_b < 10^{-6}$	$pv_b < 10^{-6}$	$pv_a = 0.764$ $pv_b = 0.430$ $pv_c = 0.804$
***p*-values—BEVs** **	$pv_a = 0.455$ $pv_b = 5.4 \times 10^{-5}$	$pv_b < 10^{-6}$	$pv_a = 0.175$ $pv_b = 0.144$ $pv_c = 0.188$

* CoG_z: height of the centre of gravity, h_r: roof height, a, bc: coefficients. ** pv: *p*-value.

In Figure 2 at the top, the measured centre of gravity heights are reported as a function of the roof height. Clearly, the IC vehicle data and BEV data have two different tendencies, with BEVs having a lower centre of gravity height for the same roof height with respect to IC vehicles. This is due to the batteries, which are typically located in the floor of the vehicle and have a large mass. The figure also depicts the best linear fit without an intercept obtained by a least square identification of the b coefficient. The two b coefficients reflect the lower CoG of the BEVs, with the BEVs having a coefficient 13% lower than the IC vehicles.

In the figure, four outliers are highlighted, with three referring to IC vehicles and one to BEVs. Referring to the three outliers of IC vehicles, these correspond to three hypercars. These cars have clearly been designed to minimise the centre of gravity height, and it is reasonable that they do not belong to the distribution of standard cars. The BEV outlier is a medium-size SUV with no evident difference compared to similar vehicles. For the computation of the interpolation coefficient, the values of these outliers have not been considered.

Figure 2 middle depicts the normal probability charts of the residual distributions for the two types of vehicles (outliers values have not been considered). In both cases, the residuals are well distributed around the theoretical values and they do not show any curvature, thus confirming that the order of the interpolation is suited for the data. In the bottom of the figure, the error distribution in the approximation of the centre of gravity height is reported. In about 70% of cases, the error was in the interval of ± 20 mm, and with all cases, not considering outliers, it comprised the interval ± 50 mm.

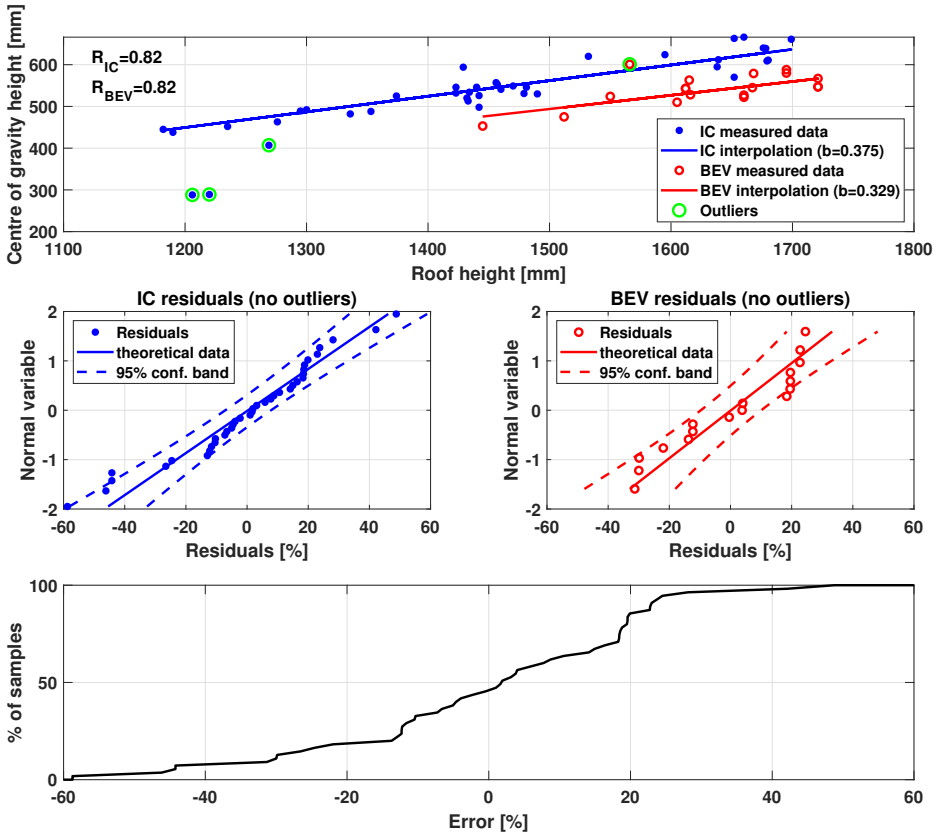

Figure 2. Centre of gravity interpolation with expression $CoG_z = b \cdot h_r$. **Top**: Linear regression for IC vehicles and BEVs (the correlation coefficient, excluding outliers, for the two series is also reported). **Middle**: Normal probability charts for the residuals of IC vehicles and BEVs. In the residuals, outliers have not been reported. **Bottom**: Distribution of the error in the centre of gravity height, excluding outliers.

6. Formulae for the Moments of Inertia

Several formulae have been proposed in the literature for the approximation of the moments of inertia. In many cases [4,6,23,26–30], formulae based on the products of the mass and geometrical dimensions, sometimes in logarithmic form, have been employed. Usually, different exponents were applied to the mass and to each geometrical dimension. The parameter exponents and coefficients have been identified on the basis of available databases. In [31,32] the authors proposed to use the formula for the computation of the moments of inertia of a uniform density parallelepiped with dimensions equal to the external dimensions of the vehicle multiplied by a single coefficient (Equations (1)–(3), with l, w, h_r length, width and roof height, respectively, and m mass). Also, a single interpolation coefficient $k = k_{xx} = k_{yy} = k_{zz} = 0.85$ could be used to satisfactory fit all of the three moments of inertia by using Equations (1)–(3) [31,32].

$$J_{xx} = k_{xx} \cdot \frac{m \cdot \left(w^2 + h_r^2\right)}{12} \tag{1}$$

$$J_{yy} = k_{yy} \cdot \frac{m \cdot \left(l^2 + h_r^2\right)}{12} \tag{2}$$

$$J_{zz} = k_{zz} \cdot \frac{m \cdot \left(l^2 + w^2\right)}{12} \tag{3}$$

In this paper, we proposed to use the formulae in Equations (1)–(3) by identifying the multiplication coefficients for each moment of inertia and separately for IC vehicles and BEVs.

In Figures 3–5, the interpolations obtained by applying Equations (1)–(3) are depicted. At the top of the figures, the interpolated values are plotted with respect to the measured values. For reference, the 45° straight line is also reported. The points appear to be well distributed around the 45° straight line. BEVs showed higher masses and higher moments of inertia with respect to IC vehicles. However, the moments of inertia grew less than the mass. This is highlighted by the coefficients k_{xx}, k_{yy} and k_{zz} that were smaller for BEVs than for IC vehicles, as reported in Table 8. The difference between the two types of vehicles is quite relevant and is due to the presence of the battery. In fact, smaller constants mean that for the same mass and dimensions, the mass of BEVs is more concentrated around the centre of gravity. This can be explained by the fact that the battery has a high density and is located mostly between the two axles, i.e., it is close to the centre of gravity. The difference was found to be lower for the roll moment of inertia than for the other moments of inertia.

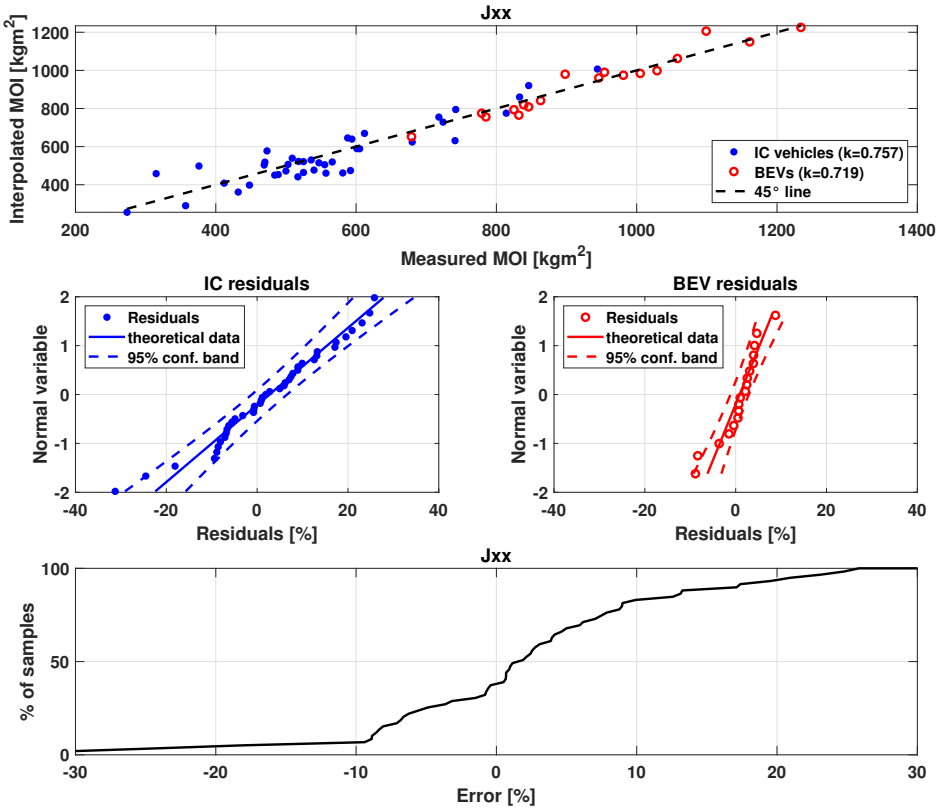

Figure 3. Roll moment of inertia interpolation using Equation (1). **Top**: Linear regression for IC vehicles and BEVs. **Middle**: Normal probability charts for the residuals of IC vehicles and BEVs. **Bottom**: Distribution of the error in the moments of inertia.

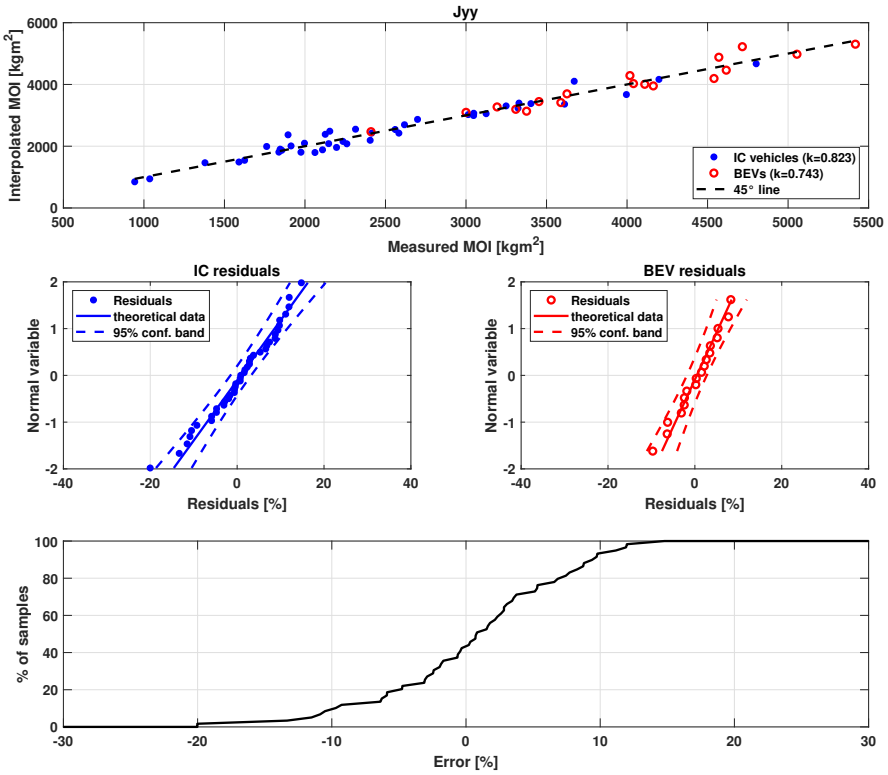

Figure 4. Pitch moment of inertia interpolation using Equation (2). **Top**: Linear regression for IC vehicles and BEVs. **Middle**: Normal probability charts for the residuals of IC vehicles and BEVs. **Bottom**: Distribution of the error in the moments of inertia.

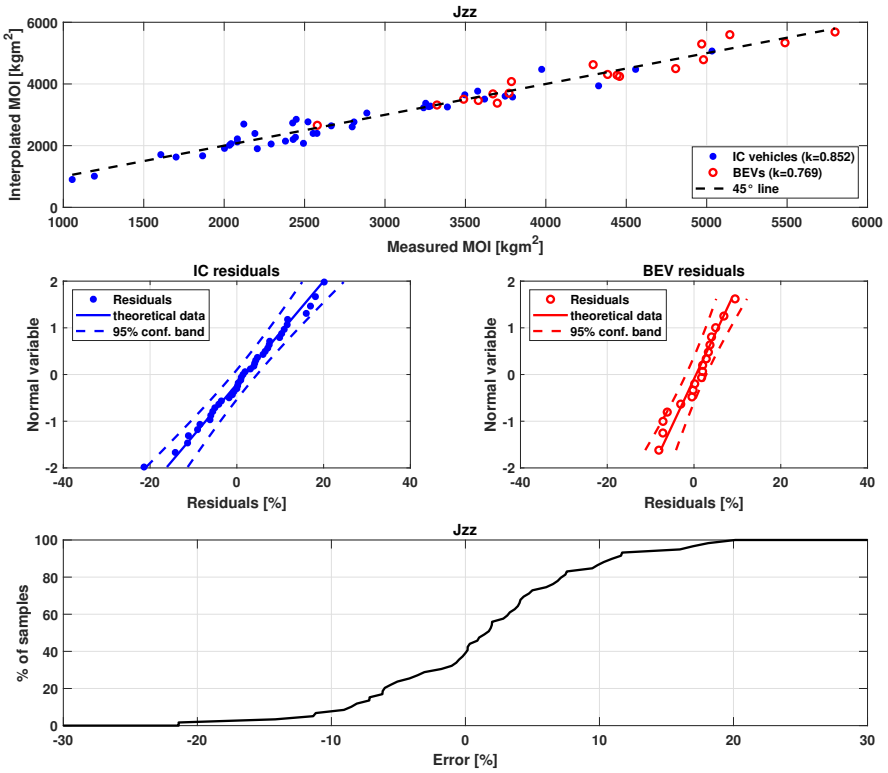

Figure 5. Yaw moment of inertia interpolation using Equation (3). **Top**: Linear regression for IC vehicles and BEVs. **Middle**: Normal probability charts for the residuals of IC vehicles and BEVs. **Bottom**: Distribution of the error in the moments of inertia.

In the middle part of Figures 1–3, the distributions of the residuals are shown. In all cases, the residuals fit well on normal distributions. Finally, at the bottom, the error distributions are reported. In all cases, about 80% of the samples had an error comprising ±10%, with almost all samples in the interval ±15%. It is worth noticing that all vehicles have been considered, and the vehicles that were outliers for the centre of gravity height appear not to be outliers for the moments of inertia.

Table 8. Coefficients of Equations (1)–(3) for IC vehicles and BEVs.

	IC Vehicles	BEVs	Difference [%]
k_{xx}	0.757	0.719	−5.0
k_{yy}	0.823	0.743	−9.7
k_{zz}	0.852	0.769	−9.7

Comparison with More Complex Formulae

The formulae of Equations (1)–(3) have a pretty simple structure with just one parameter. It can be argued that the use of more complex formulae could lead to lower interpolation errors. In [31], the authors have already shown that by referring to a more limited database of only IC vehicles, these simple formulae actually have a similar level of approximation of more complex ones. In [4], particularly complete and nonlinear formulae were proposed, which read

$$J_{ii} = 10^{k} \cdot l^{k_l} \cdot w^{k_w} \cdot h_r^{k_{h_r}} \cdot m^{k_m}, \qquad ii = xx, yy, zz \tag{4}$$

In Figures 6 and 7, the comparison between the regressions obtained by using the the simple formulae in Equations (1)–(3) and the more complex formula in Equation (4) for IC vehicles and BEVs are reported, along with the distributions of the residuals. The coefficients for Equation (4) are reported in Table 9. The figures demonstrate that the simple formulae exhibited a comparable accuracy in estimating the mass properties compared to the more complex ones, with the latter displaying slightly smaller errors. However, when the *p*-values of the estimated parameters of Equation (4) reported in Table 9 are considered, it can be observed that most of the identified parameters are not statistically meaningful. Also, the *p*-values of most of the nonsignificant parameters had similar values for both databases, even when the IC database had a much larger number of vehicles. This indicates that in most cases, the number of samples is not responsible for the nonsignificance of the parameters. Also, the *p*-values and the correlation analysis of Table 5 are in good agreement in the identification of the most significant parameters. This significance analysis shows that the additional parameters of the more complex formula hardly provided a better estimation but could imply a reduced generalisation capability of the formula, which may produce larger errors when estimating the mass properties of vehicles not pertaining to the considered database.

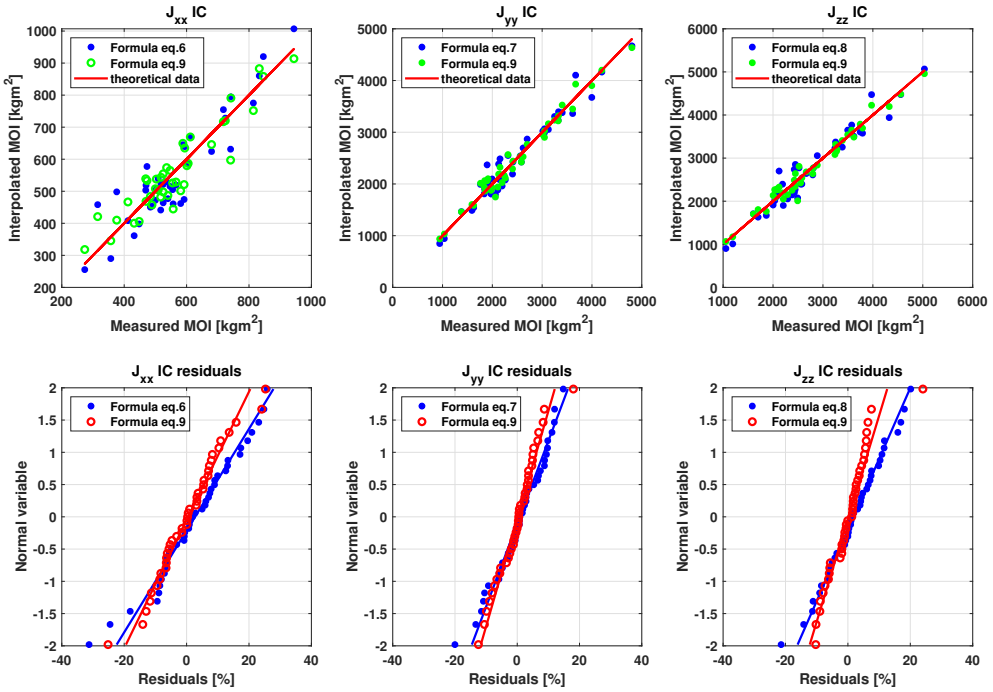

Figure 6. Comparison of the moments of inertia interpolation by considering the simple formulae in Equations (1)–(3) and the more complex formula in Equation (4) for IC vehicles. **Left**: J_{xx}. **Middle**: J_{yy}. **Right**: J_{zz}. **Top**: Regressions. **Bottom**: Normal probability charts for the residuals.

Table 9. Coefficients of Equations (1)–(3) for IC vehicles and BEVs.

Coefficients for J_{xx}					
	k	k_l	k_w	k_{h_r}	k_m
IC (values)	0.048	−0.231	−0.662	0.576	1.218
IC (p-values)	0.983	0.547	0.356	0.014	$<10^{-4}$
BEV (values)	−6.835	0.297	1.078	0.860	0.712
BEV (p-values)	0.002	0.683	0.254	0.017	0.002
Coefficients for J_{yy}					
	k	k_l	k_w	k_{h_r}	k_m
IC (values)	−4.276	1.391	−0.708	0.353	1.182
IC (p-values)	0.004	$<10^{-4}$	0.102	0.01	$<10^{-4}$
BEV (values)	−7.929	0.832	1.340	0.202	1.027
BEV (p-values)	0.005	0.392	0.273	0.628	0.001
Coefficients for J_{zz}					
	k	k_l	k_w	k_{h_r}	k_m
IC (values)	−3.724	1.223	−0.542	0.233	1.157
IC (p-values)	0.012	$<10^{-4}$	0.217	0.094	$<10^{-4}$
BEV (values)	−7.104	1.121	0.572	0.391	1.0244
BEV (p-values)	0.008	0.230	0.622	0.340	0.001

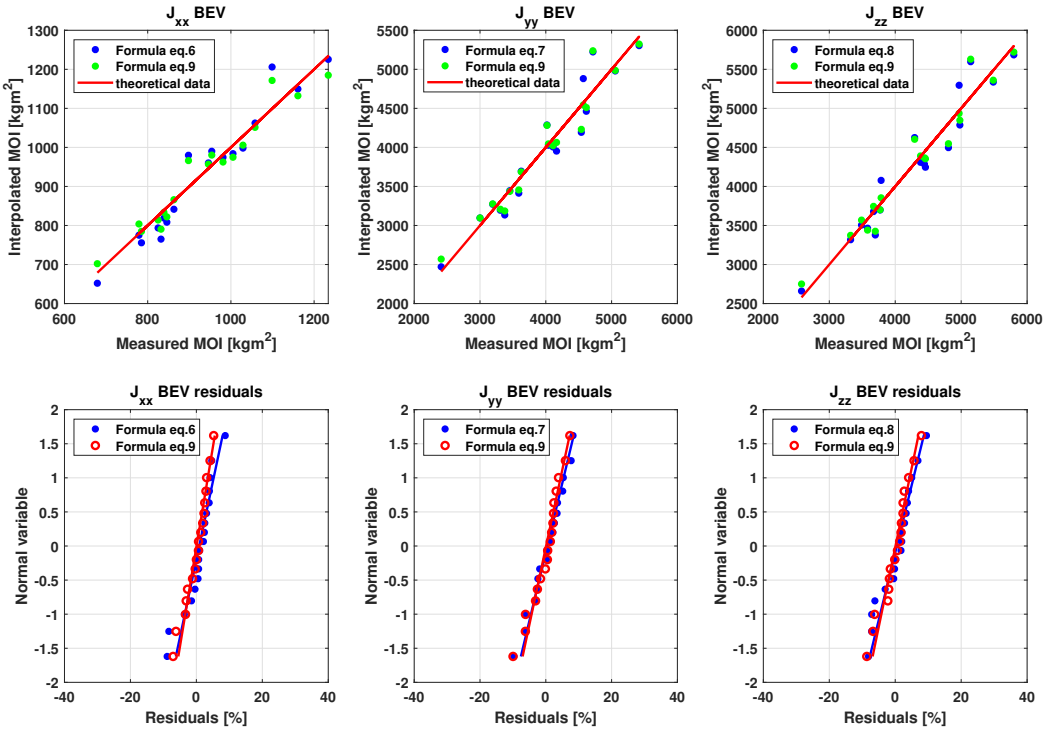

Figure 7. Comparison of the moments of inertia interpolation by considering the simple formulae in Equations (1)–(3) and the more complex formula in Equation (4) for BEVs. **Left**: J_{xx}. **Middle**: J_{yy}. **Right**: J_{zz}. **Top**: Regressions. **Bottom**: Normal probability charts for the residuals.

7. Conclusions

In this paper, with the aim of providing reliable mass properties for accident reconstruction in particular, the centre of gravity height and the moments of inertia of internal combustion and electric vehicles have been investigated. A database of vehicle mass properties measured at the Politecnico di Milano comprising vehicles form 1997 to 2023 has been employed to derive the empirical formulae for estimating the considered mass properties. The mass properties were estimated as functions of easily available vehicle data.

Firstly, a simple correlation analysis has shown that the moments of inertia can be estimated from the values of vehicle mass, length, width and roof height, while the centre of gravity height was shown to be a function of the roof height only.

For the estimation of the centre of gravity height, a simple proportional constant with respect to the roof height was found to be sufficient. An error of less than $\pm$20 mm could be obtained in about the 70% of cases, with maximum error being less than 50 mm.

The estimation of the moments of inertia require the mass and external dimensions of the vehicle. A simple formula based on the expression of the moments of inertia of a constant density parallelepiped multiplied by a constant has been proposed. This formula, which is a function of only one parameter to be tuned on the basis of available measurements, has shown to be reasonably accurate in predicting the desired values. In about 80% of the cases, the error was $\pm$10%, while the maximum error was below 15%.

One of the main results of the paper is the comparison between the mass properties of internal combustion and electric vehicles. Electric vehicles show higher values of mass but lower values of the centre of gravity height and proportionally lower values of the moments of inertia. The differences in the mass properties of the two types vehicles is quite relevant, and specific parameters should be used for the approximation formulae. In fact, the multiplying constants in the proposed interpolation formulae differed by 5% to 13% for the two types of vehicles. The comparison between internal combustion and electric vehicles has also shown that as vehicles evolve, the mass distribution changes as well. Therefore, future measurements can be added to the current database and to the analysis.

Finally, the proposed simple formulae were compared with more complex formulae taken from the literature. The comparison shows that the simple formulae have a comparable level of accuracy in the estimation of the moments of inertia with respect to the more complex ones. Also, a statistical significance analysis has shown that adding more interpolation parameters leads to the identification of parameters with a low level of significance that may reduce the error with respect to the considered database but could reduce the generalisation capabilities of the formulae.

The formulae presented in this paper provide a convenient and reasonably precise method for estimating the primary mass properties of a vehicle. Such estimations are particularly valuable in accident reconstruction, where more precise data are often not readily accessible, and poorly estimated mass properties can result in significant errors in the reconstructed velocities and trajectories of the vehicles involved in the accident.

Author Contributions: Conceptualization, G.P., G.M. and M.G.; methodology, G.P.; software, G.P.; validation, G.P., G.M. and M.G.; formal analysis, G.M.; investigation, G.P. and M.G.; resources, G.M. and M.G.; data curation, G.P.; writing—original draft preparation, G.P. and M.G.; writing—review and editing, G.M.; visualization, G.P.; supervision, G.M. and M.G.; project administration, G.M. and M.G.; funding acquisition, G.M. and M.G. All authors have read and agreed to the published version of the manuscript.

Funding: This research received no external funding.

Data Availability Statement: Data is unavailable due to confidentiality.

Conflicts of Interest: The authors declare no conflicts of interest.

References

1. World Health Organization. *Global Status Report on Road Safety 2018*; World Health Organization: Geneva, Switzerland , 2018.
2. Steffan, H. Accident reconstruction methods. *Veh. Syst. Dyn.* **2009**, *47*, 1049–1073. [CrossRef]
3. Brach, M.; Brach, R.M.; Mason, J. *Vehicle Accident Analysis and Reconstruction Methods*, 3rd ed.; SAE International: Warrendale, PA, USA, 2022.
4. Allen, R.W.; Klyde, D.H.; Rosenthal, T.J.; Smith, D.M. *Estimation of Passenger Vehicle Inertial Properties and Their Effect on Stability and Handling*; SAE International: Warrendale, PA, USA, 2003.
5. Vella, A.D.; Vigliani, A. Research on the Longitudinal Dynamics of an Electric Scooter. *SAE Int. J. Veh. Dyn. Stab. NVH* **2022**, *7*, 35–51. [CrossRef]
6. MacInnis, D.D.; Cliff, W.E.; Ising, K.W. *A Comparison of Moment of Inertia Estimation Techniques for Vehicle Dynamics Simulation*; SAE International: Warrendale, PA, USA, 1997.
7. Gobbi, M.; Mastinu, G.; Previati, G. A method for measuring the inertia properties of rigid bodies. *Mech. Syst. Signal Process.* **2011**, *25*, 305–318. [CrossRef]
8. Lund, Y.I.; Bernard, J.E. Analysis of Simple Rollover Metrics. *SAE Trans.* **1995**, *104*, 434–450
9. Marine, M.C.; Wirth, J.L.; Thomas, T.M.; Engineering, T. *Characteristics of On-Road Rollovers*; SAE International: Warrendale, PA, USA, 1999.
10. Dong, G.M.; Zhang, N.; Du, H.P. Investigation into untripped rollover of light vehicles in the modified fishhook and the sine manoeuvres, part II: Effects of vehicle inertia property, suspension and tyre characteristics. *Veh. Syst. Dyn.* **2011**, *49*, 949–968. [CrossRef]
11. BS-ISO. BSI Standards Publication Road Vehicles-Determination of Centre of Gravity. 2011. Available online: https://www.iso.org/standard/52978.html (accessed on 10 June 2024).
12. SAWE. *SAWE Weight Engineers Handbook*; Society of Allied Weight Engineers: Los Angeles, CA, USA, 2011.
13. Schedlinski, C.; Link, M. A survey of current inertia parameter identification methods. *Mech. Syst. Signal Process.* **2001**, *15*, 189–211. [CrossRef]
14. Zhang, L.; Wang, M.; Lin, J.; Liu, P. A demodulation algorithm for processing rotational inertia signals using a torsion pendulum method based on differentiation and resonance frequency analysis. *Meas. Sci. Technol.* **2020**, *32*, 025005. [CrossRef]
15. Li, T.; Shangguan, W.B.; Yin, Z. Error analysis of inertia parameters measurement for irregular-shaped rigid bodies using suspended trifilar pendulum. *Measurement* **2021**, *174*, 108956. [CrossRef]
16. Andreatta, D.A.; Heydinger, G.J.; Bixel, R.A.; Coovert, D.A. *Inertia Measurements of Large Military Vehicles*; SAE International: Warrendale, PA, USA, 2001.
17. Suhaimi, K.; Risby, M.S.; Tan, K.S.; Syafiq, M.S.A.; Hafizi, N.M. Heavy military land vehicle mass properties estimation using hoisting and pendulum motion method. *Def. Sci. J.* **2019**, *69*, 550–556.

18. Previati, G. Large oscillations of the trifilar pendulum: Analytical and experimental study. *Mech. Mach. Theory* **2021**, *156*, 104157. [CrossRef]
19. Antony-Best. Moments of Inertia and CoG. Available online: https://www.abdynamics.com/en/products/measurement-systems/moments-of-inertia-and-c-of-g/spmm-5000e-mims-upgrade (accessed on 10 June 2024).
20. Zhu, T.; Li, F. Experimental investigation and performance analysis of inertia properties measurement for heavy truck cab. *Adv. Mech. Eng.* **2015**, *7*, 1687814015618629. [CrossRef]
21. Wegener, D. Vehicle inertia measurement machine (VIMM). In Proceedings of the Society of Allied Weight Engineers 71st Annual Conference, Virginia Beach, Virginia, 20–22 May 2012.
22. Brancati, R.; Russo, R.; Savino, S. Method and equipment for inertia parameter identification. *Mech. Syst. Signal Process.* **2010**, *24*, 29–40. [CrossRef]
23. Fundowicz, P.; Sar, H. Estimation of mass moments of inertia of automobile. In Proceedings of the 11th International Science and Technical Conference Automotive Safety, AUTOMOTIVE SAFETY 2018, Casta, Slovakia, 18–20 April 2018; IEEE: Piscataway, NJ, USA, 2018; pp. 1–6.
24. Holjevac, N.; Cheli, F.; Gobbi, M. Multi-objective vehicle optimization: Comparison of combustion engine, hybrid and electric powertrains. *Proc. Inst. Mech. Eng. Part D J. Automob. Eng.* **2020**, *234*, 469–487. [CrossRef]
25. Zhang, Q.; Hou, J.; Hu, X.; Yuan, L.; Jankowski, Ł.; An, X.; Duan, Z. Vehicle parameter identification and road roughness estimation using vehicle responses measured in field tests. *Measurement* **2022**, *199*, 111348. [CrossRef]
26. Heydinger, G.J.; Bixel, R.; Garrott, W.R.; Pyne, M.; Howe, J.G.; Guenther, D. *Measured Vehicle Inertial Parameters-NHTSA's Data Through November 1998*; SAE International: Warrendale, PA, USA, 1999.
27. Garrott, W.R.; Monk, M.W.; Chrstos, J.P. *Vehicle Inertial Parameters-Measured Values and Approximations*; SAE International: Warrendale, PA, USA, 1988.
28. Garrott, W.R. *Measured Vehicle Inertial Parameters -NHTSA's Data through September 1992*; SAE International: Warrendale, PA, USA, 1993.
29. Riede, P.M.; Leffert, R.L.; Cobb, W.A. *Typical Vehicle Parameters for Dynamics Studies Revised for the 1980's*; SAE International: Warrendale, PA, USA, 1984.
30. Noon, K. *Engineering Analysis of Vehicle Accidents*; CRC Press: Boca Raton, FL, USA, 1994.
31. Previati, G.; Mastinu, G.; Gobbi, M. Investigation on the mass properties of cars. In Proceedings of the 78th SAWE International Conference on Mass Properties Engineering, Norfolk, VI, USA, 18–23 May 2019.
32. Gobbi, M.; Mastinu, G.; Pennati, M.; Previati, G. InTenso+ System: Measured Centre of Gravity Locations and Inertia Tensors of Road Vehicles. In Proceedings of the ASME 2014 International Design Engineering Technical Conferences and Computers and Information in Engineering Conference. Volume 3: 16th International Conference on Advanced Vehicle Technologies; 11th International Conference on Design Education; 7th Frontiers in Biomedical Devices, Buffalo, NY, USA, 17–20 August 2014.
33. Wiegand, B.P. Automotive mass properties estimation. In Proceedings of the SAWE 69th Annual Conference, Boston, MA, USA, 1–5 May 2010; pp. 1–103.
34. Liang, J.; Lu, Y.; Yin, G.; Fang, Z.; Zhuang, W.; Ren, Y.; Xu, L.; Li, Y. A Distributed Integrated Control Architecture of AFS and DYC Based on MAS for Distributed Drive Electric Vehicles. *IEEE Trans. Veh. Technol.* **2021**, *70*, 5565–5577. [CrossRef]
35. Previati, G.; Gobbi, M.; Mastinu, G. Measurement of the mass properties of rigid bodies by means of multi-filar pendulums—Influence of test rig flexibility. *Mech. Syst. Signal Process.* **2019**, *121*, 31–43. [CrossRef]
36. Previati, G.; Gobbi, M.; Mastinu, G. Method for the Measurement of the Inertia Properties of Bodies with Aerofoils. *J. Aircr.* **2012**, *49*, 444–452. [CrossRef]
37. Spearman, C. The Proof and Measurement of Association between Two Things. *Am. J. Psychol.* **1904**, *15*, 72. [CrossRef]